Geochimica et Cosmochimica Acta
November 2008, Volume 72, Issue 22, Pages 5416-5430
http://dx.doi.org/10.1016/j.gca.2008.08.021

Mercury sources and transformations in a man-perturbed tidal estuary; the Sinnamary Estuary, French Guiana

B. Muresan[1], D. Cossa[1, *], M. Coquery[2], S. Richard[3]

[1] Institut français de recherche pour l'exploitation durable de la mer (IFREMER), BP 21105, F.44311 Nantes cedex 3, France (EU)
[2] Centre national du machinisme agricole, du génie rural et des eaux et forêts (CEMAGREF), BP 220, F.69336 Lyon cedex 9, France (EU)
[3] Laboratoire de recherche en environnement barrage de Petit-Saut (HYDRECO), BP 823, F.97388 Kourou, French Guiana (EU)

*: Corresponding author : D. Cossa, email address : Daniel.Cossa@ifremer.fr

Abstract:

The distribution, partition and speciation of mercury (Hg) were studied along the redox gradient of an anthropogenically perturbed tropical estuary, the Sinnamary Estuary in French Guiana. This system is a partially mixed estuary characterized by an anoxic freshwater end-member, while the marine end member consists of the Amazon Plume.
The set up of an artificial oxygenation system in the anoxic freshwater end-member generates sharp gradients of major chemical species (iron, sulfides, etc.) coupled with intense organic matter (OM) turnover. The coexistence of oxygenated waters and dissolved sulfides in an organic rich environment depicts the Upper Sinnamary Estuary (USE: part of Sinnamary Estuary under the tidal influence but upstream of the salt intrusion) as a potential site for Hg methylation. The concentrations of all mercurial species (HgT) in the unfiltered samples (HgTUNF), in the dissolved (HgTD) and particulate (HgTP) phases of the USE average 11 $\pm$ 3, 6 $\pm$ 2 and 5 $\pm$ 3 (i.e. 600 $\pm$ 200 pmol g^{-1}) pmol L^{-1} respectively. Average concentrations of monomethylmercury (MMHg) in the unfiltered (MMHgUNF), dissolved (MMHgD) and particulate (MMHgP) phases were 3.7 $\pm$ 1.0, 2.0 $\pm$ 0.9 and 1.8 $\pm$ 1.2 (i.e. 220 $\pm$ 130 pmol g^{-1}) pmol L^{-1} respectively. Water oxygenation and sulfides concentrations emerged to play a critical role in controlling MMHg levels. Additionally, iron cycling, acid-base mechanisms, and edox-dependent processes were involved in the MMHg partitioning between phases. Overall, the USE constitutes a biogeochemical reactor that gathers partitioning and methylation processes. The permanent MMHg inputs from the anoxic freshwater end-member combined with the intense endogenous Hg methylation ensures high MMHg levels in both dissolved and particulate phases. To illustrate, the USE exports 60 $\pm$ 20 % more MMHgUNF than it imports: 5.5 $\pm$ 0.7 vs. 3.5 $\pm$ 1.2 kg y^{-1}.

Keywords: Estuary; Reservoir; Mercury; Redox; Speciation; Partitioning

1. Introduction

Estuaries define transitional environments of active biogeochemical transformations. The chemical and physical gradients characterizing these continent-ocean interfaces affect the cycle of numerous metals (Boyle *et al*., 1977; Mantoura *et al*., 1978; Sholkovitz *et al*., 1978; Boughriet *et al*., 1992; Mota *et al*., 2005). Among those, mercury (Hg) transformations are particularly important. Its multiple valence states and chemical associations (with thiol or sulfide groups) are common in natural conditions (Baeyens and Leemarkers, 1998; Dyrssen and Wedborg, 1991; Cossa and Gobeil, 1996; Coquery *et al*., 1997). The Hg cycle also involves biologically mediated processes such as reduction / oxidation or methylation / demethylation (e.g., Choi *et al*., 1994; Heyes *et al*., 2006; Whalin *et al*., 2007).

In the aquatic environment, monomethylmercury (MMHg) is the form of greatest concern since it collects in organisms (bioaccumulates) and concentrates up food chains (biomagnifies). MMHg concentration maxima are generally correlated with redox transition zones containing sulfate-reducing bacteria (SRB) which are thought to be the key methylating agents (e.g., Jensen and Jernelov, 1969; Gilmour et al., 1992; King et al., 1999; Benoit et al., 2003; Bisinoti and Jardim, 2005). Exploration of redox dependant and biologically driven mechanisms is of great significance for predicting the distribution and speciation of Hg inputs to freshwater lakes and reservoirs, including coastal sediments, the ocean, the atmosphere, and their living organisms.

In temperate and cold regions, the potential methylation of inorganic Hg to MMHg has given rise to numerous studies (e.g. Compeau and Bartha, 1984, 1985; Mason *et al*., 1993; Benoit *et al*., 1998; Mason *et al*., 1999; Sunderland *et al*., 2004; Rodriguez *et al*., 2004; Stoichev *et al*., 2006). In contrast, Hg behavior in tropical estuaries is very poorly known (Guimaraes *et al*., 2000a and b; Roulet *et al*., 1998a, 2000; Sergio *et al*., 2006). The paucity of data is all the more manifest when considering tropical estuaries that undergo hypolimnetic discharges from a stratified man-made lake. Consider, we dammed over half of the world's streams at unprecedented rates of one per hour, and at unprecedented scales of over 45,000 dams more than 15 m high (World Commission on Dams, 2000). Almost all of these dams display periods of stratification and development of an anoxic hypolimnion in the deepest part of their reservoirs (International Commission on Large Dams, 2003). Stratified reservoirs exhibit a great potential for increased MMHg production in the hypolimnion of their water column and/or in the anoxic zone of their sediments (Parks *et al*., 1989; Bloom and Effler, 1990; Watras *et al*., 1994; Jacobs *et al*., 1995). Discharged waters also contain high levels of organic matters (OM) and hydrogen sulfides (ΣH_2S). Build up of favorable methylating conditions (intense microbial activity coupled with reduced water oxygenation) downstream of the reservoirs supports the formation of endogenous MMHg. Accordingly, the environmental impact of the rivers, estuaries and other water bodies that undergo hypolimnetic discharges is far from negligible.

The main goal of this paper is to test the hypothesis offered by Benoit et al. (2003) stating that the extent of Hg methylation would be a function of sulfides levels, as this is the ligand controlling Hg speciation in solution in low oxygen zones where SRB are active. Furthermore, the same authors pointed to the difficulty to ascertain from the field data which among Fe, S and OM is the dominant solid phase binding Hg in the environment. Therefore, we probed the magnitude of the effect of these species on the Hg dynamics between the dissolved and the particulate phases. To reach this goal, we appraised the methylation potential of a tropical water bodies that undergo hypolimnetic discharges. We addressed the following questions (i) What is the role of hypolimnetic discharges on the estuarine Hg cycle? (ii) Is there a redistribution of Hg species between the dissolved and particulate phase? (iii) What are the roles of OM and iron in the redistribution of Hg between phases? (iv) What is the importance of the in situ methylation with respect to external sources of MMHg? and (v) Which parameters and/or processes govern the production of MMHg in these aquatic environment? We address these questions in the Sinnamary Estuary (French Guiana, Fig. 1). An estuary that undergoes permanent hypolimnetic discharges from the hydroelectric reservoir of Petit-Saut.

2. The Sinnamary Estuary

The Sinnamary Estuary spans over 70 km from the dam of the artificial reservoir of Petit-Saut (5°04' North, 53°03' West) to the Atlantic Ocean (Fig. 1). Some minor creeks contribute to the total water discharge to the ocean. The residence time of waters is between 24 and 48 hours (HYDRECO data). The tidal amplitude ranges from a few centimeters near the dam to a maximum close to 3 m at the

mouth of the estuary during spring tide (Amouroux, 2003). However, the salt intrusion never exceeds a few km beyond the village of Sinnamary. We called the freshwater portion the Upper Sinnamary Estuary (USE) and the saline portion the Lower Sinnamary Estuary (LES). The USE is *circa* 50 m width, its depth at mid-width varies between 5 and 10 m and its course displays an overall slope of 0.03 m km^{-1}. Except for local falls (named "Sauts"), where the water stream was turbulent, the circulation pattern of the USE was characterized by a near-laminar flow regime. In its water column, the high volumes of hypolimnetic discharges and the low-depth water bottom set the measured parameters stable with depth.

Between 1989 and 1994, the construction of the hydroelectric dam of Petit-Saut took place. The filling of the reservoir generated major modifications in the water chemistry of the USE. Initially, the waters were warm, acidic, only slightly conductive, oxygenated, nutrient poor and relatively homogenous (Horeau *et al*., 1998). As a result of the Petit-Saut reservoir stratification, the USE started to convey mineralized waters related to elevated amounts of OM and reduced species. To maintain dissolved oxygen concentrations that are compatible with aquatic life, an aeration system was set up in the outflow from the dam turbines. Nonetheless, strong oxygen consumption remained apparent within the estuary (up to 0.1 mmol L^{-1} of 5-day biological oxygen demand according to Richard *et al*., 1997).

3. Material and Methods

3.1. Sampling campaigns

Samples from the Sinnamary Estuary were collected during five campaigns that took place in March-April 2003, January-February 2004, May-June 2004, November-December 2004 and February-March 2005. The sampling campaigns, designated as Matoutou 1, 2, 3, 4 and 5, reflected the major seasons of the guianese climate (Tab. 1). Those are the short wet season (from November to February), the short dry season (from February to April), the long wet season (April to July) and the long dry season (from July to November). During the Matoutou campaigns, from 200 m downstream of the dam (5°04.01'N - 53°03.26'W) to the saline gradient (5°26.03'N - 52°59.62'W), the USE was invariably sampled at the same eight stations: Pas., Ker., Cha., Ven., Bra., Com., Deg. and Sin. (i.e., Passerelle, Kerenrock, Chapeau, Venus, Bravo, Combi, Degrad and the village of Sinnamary, respectively) (Fig. 1). The Sin. station was the geographical reference point used to distinguish the USE from the LES. The locations of the sampling stations were chosen to provide a comprehensive assessment of Hg species transformations in the USE with respect to important ancillary parameters such as OM and dissolved iron.

Additional sampling for water took place on a weekly basis between March 2003 and December 2004 at the tailrace (the downstream part of a dam where the impounded water re-enters the river) of the turbines. The tailrace station (noted Tail., 5°03.89'N - 53°02.85'W) reflected the average conditions of the hypolimnetic dam discharges (approximately 180 m^3 s^{-1}). The oxygenated freshwaters tributaries of the USE were sampled during Matoutou 2, 3, 4 and 5 sampling campaigns (Tab. 1). Four main tributaries were investigated, namely the Gregoire, Chapeau, Venus and Saulnier creeks. These accounted for about one fifth of the total freshwater flow to the USE (approximately 50 m^3 s^{-1}).

3.2. Sample collection

Subsurface water samples were collected 20 cm below the air-water interface (AWI) by immersing an acid washed Teflon bottle (FEP) with a gloved hand. Analyses of dissolved gaseous mercury (DGM) were performed within 2 hours of collection at the dam field laboratory (HYDRECO). The sum of all Hg species (unfiltered HgT or HgT_{UNF}) along with the dissolved (HgT_D) and reactive (HgR_{UNF}) fractions were processed the same day. Aliquots were kept to determine MMHg in the unfiltered ($MMHg_{UNF}$), dissolved ($MMHg_D$) and the particulate ($MMHg_P$) phases. Water samples were filtered using hydrophilic Teflon membranes (0.45 µm pore size, 45 mm diameter, LCR®, Millipore) and acidified with 0.5 % (v/v) HCl (Suprapur®, Merck). The filtrates were operationally defined as "dissolved" but there is no claim being made that filtration through 0.45 µm is a true separation of suspended and dissolved forms of Hg. Used filters (particulate samples) and corresponding filtered solutions were ultimately double bagged and stored at –20 °C in dark conditions until analysis.

3.3. Sample analysis

3.3.1. Ancillary parameters

The pH, dissolved oxygen, conductivity and redox were recorded in situ with a YSI 600XLM multiparameter probe. Total sulfides (ΣH_2S) "dissolved" (<0.45 µm) sulfate (SO_4) and dissolved iron (FeT_D including both Fe^{II} and Fe^{III} measurements) were measured by colorimetry (Merck, 2001). Samples for organic carbon in the unfiltered (TOC) and the dissolved (DOC) phases were analyzed by IR spectroscopy after oxidative or acidic digestion of the samples.

3.3.2. Mercurial speciation in water and particles

All Hg species were quantified using cold vapor atomic fluorescence spectrometry (CVAFS). HgT was determined according to Bloom and Fitzgerald (1988), by the formation of volatile elemental Hg (released by $SnCl_2$ reduction, after 30 minutes of acidic BrCl oxidation) and preconcentration on a gold trap. HgR (the easily reducible fraction) was obtained by direct reduction with $SnCl_2$ (pH 1). Unfiltered samples were analyzed for dissolved gaseous mercury (DGM mainly Hg^0) by sparging for 20 min with Hg-free argon at 200 mL min^{-1}. The detection limits, defined as 3.3 times the standard deviation of the blanks, were usually 0.05 pmol L^{-1} for HgT and HgR, and 25 fmol L^{-1} for DGM. The sample volume analyzed for HgT, HgR and DGM was between 50 and 100 mL. The relative standard deviation, calculated on five replicate samples of about 0.5 pmol L^{-1}, was lower than 10 %. The mean recovery and variance associated with the accuracy for HgT determinations were 93 $\pm$ 5 % and were regularly checked, using the reference material (ORMS-3) from the National Council of Canada as certified reference material (CRM). MMHg was determined in the unfiltered ($MMHg_{UNF}$) and dissolved ($MMHg_D$) phases using the method proposed by Bloom (1989) and modified by Liang *et al*. (1994) and Leermakers *et al*. (2001). The water samples were stored with 0.5 % (v/v) HCl, which is a reliable method for a 3 week storage period (Parker and Bloom, 2005). MMHg in acidified water was extracted by CH_2Cl_2 and then transferred into 40 mL of Milli-Q water by evaporating the organic solvent. The aqueous solutions were analyzed for MMHg by gas chromatography after ethylation and adsorption / desorption on a Tenax® column. For HgT_P and $MMHg_P$ in suspended particulate matters (SPM), an acidic dissolution (with concentrated HCl / HNO_3) of the filtered particles took place before the procedures described previously. Detection limits for MMHg were 0.01 pmol L^{-1} and 0.005 pmol g^{-1} for respectively a 100 mL water and 200 mg solid sample. Precision was bellow 10 % for all analyses. Using the available reference material (IAEA-405), the accuracy of the method was estimated to be 91 $\pm$ 8 % recovery. The detailed procedure is given by Cossa *et al*. (2002 and 2003).

3.4. Modeling the mercurial scavenging and complexation

3.4.1. Modeling the mercurial scavenging

The scavenging of dissolved Hg (Q_a, kg) was formulated as the product of the average trapping coefficient of Hg (k, no units) and the local consumption of scavenging agent (Q_s, kg):

$$Q_a = k\, Q_s$$

The equilibrium between dissolved Hg, ligands and suspended matters is usually based on the surface complexation theory (Stumm *et al*., 1980; Westall, 1987; Dzombak and Morel, 1990). In this approach, the high affinity of Hg for sulfides, oxyhydroxides, and OM ensures that equilibrium between the dissolved and the solid phases is quickly achieved (Morel *et al*., 1998). Hence, dissolved Hg levels are essentially driven by the available quantity of sorbent:

$$\Delta[A] = -\, k\, \Delta[S] \quad ; \quad k = \frac{[SA]}{K_{ads}\,[S]^2}$$

$$S + A \Leftrightarrow SA \quad ; \quad K_{ads} = \frac{[SA]}{[S]\,[A]}$$

where [S] is the particulate fraction of the sorbent (µmol L^{-1}), [A] is the concentration of dissolved Hg (pmol L^{-1}) and [SA] is the concentration of the Hg-sorbent bounded complexes (pmol L^{-1}). Calling [D] the dissolved fractions of the sorbent (µmol L^{-1}) and considering that the total amount of sorbent in the USE remains relatively unchanged (this was testified for total S, FeT and TOC):

$$k = -\frac{\Delta[A]}{\Delta[S]} \approx \frac{\Delta[A]}{\Delta[D]}$$

One could thus approach the trapping coefficient (k) by measuring the concentrations of dissolved Hg along with that of dissolved scavenging agent (i.e. ΣH_2S, FeT_D and DOC).

3.4.2. Modeling the mercury complexation

The speciation code line Winderemere Humic Aqueous Model (WHAM 6; Tipping, 2002) was used to probe the speciation of dissolved and particulate strongly complexed Hg (Hg_{SC} = HgT – HgR – MMHg; Mason *et al*., 1993), and dissolved MMHg in the USE. In the WHAM 6 approach, humic compounds are represented by hypothetical size-homogenous, rigid, molecules, which carry proton-dissociating groups that can bind metal ions either singly or as bidentate pairs. Inputs to the WHAM 6 speciation code line were in compliance with Goulet et al. (2007). Briefly, inputs consisted of the pH, [HgT_{SC}], [$MMHg_D$], [ΣH_2S], [Al], [Fe], [Mn] and major ions, as well as estimates of humic (HA) and fulvic (FA) acid concentrations. To estimate [HA] and [FA], we assumed that DOC contained 50% C (Buffle, 1988) and that all DOC was humic substances with a ratio of [FA]:[HA] of 9:1 (Malcolm, 1985). The WHAM 6 thermodynamic databases was updated with the equilibrium constants for the systems Hg-sulfide-polysulfide and MeHg-sulfide given in Goulet et al. (2007), and dissolved elemental sulfur ($S^0_{(aq)}$) and $MeHg^+$ were added as components in the code. The formation constants recommended by the National Institute of Standards and Technology (NIST, 2004) and Powell et al. (2005) for Hg complexation with OH^-, Cl^-, NO_3^- and CO_3^{2-} were also used to update the WHAM 6 databases. The intrinsic equilibrium constant for Hg MMHg complexes with FA and HA used in the calculations were those estimated by Tipping (2007).

4. Results and Discussion

4.1. Chemical characteristics of the waters

Figure 2 displays the transects for pH, redox (Eh), conductivity, particulate organic carbon (POC), dissolved organic carbon (DOC), oxygen (O_2), iron (FeT_D) and sulfides (ΣH_2S) obtained during the Matoutou 1, 2, 3, 4 and 5 campaigns at the nine (Tail., Pas., Ker., Cha., Ven., Bra., Com., Deg. and Sin.) stations. The pH in the USE was plainly acidic (5.7 ± 0.3; average ± SD). The longitudinal distribution of Eh increased with distance from the dam (from 150 to 400 mV) while O_2 and conductivity showed patterns of gradual decrease and low levels (approximately 0.1 mmol L^{-1} and < 30 µS cm^{-1}, respectively) were reached between Com. and Sin. stations. Since Eh is a proxy of the concentration of reducing agents, we observed a gradual oxidation of the water masses along their course to the Atlantic Ocean.
De Junet (2004) stated that carbon exportations downstream of the dam in 2003, *circa* 80 10^9 g C y^{-1}, were dominated by volatile compounds (50 10^9 g C y^{-1} mostly as CO_2 and CH_4). During the Matoutou sampling campaigns, TOC in the USE averaged 0.47 ± 0.02 mmol L^{-1} of which 90 % (0.41 ± 0.04 mmol L^{-1}) was DOC (Fig. 2). With distance from the dam, we observed a gradual increase of POC (from < d.l. to 0.08 mmol L^{-1}) to the detriment of DOC (from 0.48 to 0.37 mmol L^{-1}). Hence, an inverse behavior was reported with the O_2 up to saturation (%) {r^2 = 0.45; O_2 (%) = -600 $[POC]_{mmol\ L\text{-}1}$ + 93}. The maximum of OM mineralization (minimum of POC) was located within the first kilometers downstream of the Petit-Saut dam and developed during the wet seasons. Quantitatively, the

mineralization of autochthonous particulate OM in the USE represented 30 % of its gaseous CO_2 and CH_4 emissions (De Junet, 2004).

In the USE, FeT_D averaged 8 ± 6 µmol L^{-1}. The highest concentrations (17 ± 6 µmol L^{-1}) were measured at the tailrace (Fig. 2) and corresponded to up to 7000 tons y^{-1} of FeT_D discharged downstream of the dam. The FeT_D negatively correlated with redox (r^2 = 0.62; $[FeT_D]_{\mu mol\ L\text{-}1}$ = -0.08 Eh_{mV} + 30). Simultaneous removal of both iron and oxygen from the dissolved phase suggested a partial oxidation of FeT_D (presumably Fe^{2+}) to Fe oxyhydroxides. Maximum of Fe^{III} concentrations (around 50 µmol L^{-1}) were located in the vicinity of the Ker. station *circa* 20 km downstream of the dam (15 ± 8 µmol L^{-1} of Fe^{II}). The ΣH_2S concentrations in the USE ranged from < 0.1 to 2 µmol L^{-1} (Fig. 2) and averaged 0.7 ± 0.5 µmol L^{-1}. The ΣH_2S concentrations markedly decreased in the first kilometers downstream of the dam. Formation of sulfates through in situ ΣH_2S oxidation coupled with locally reducing (< 200 mV) and suboxic (< 0.1 mmol L^{-1} O_2) conditions would contribute to sustain the USE endogenous activity of SRB. This was confirmed by water and biofilms incubation experiments that developed substantial SRB concentrations (Jorand pers. com.).

4.2. Mercury inputs to the Estuary

4.2.1. The role of the dam

HgT_{UNF} concentrations at the Tail. station varied between 3.8 pmol L^{-1} (June 2003) and 27.9 pmol L^{-1} (July 2004; Fig. 3). Average HgT_{UNF} concentration was 13 ± 5 pmol L^{-1} of which about 60 % (8 ± 2 pmol L^{-1}) were HgT_D (Tab. 2). We observed (Fig. 3) a trend towards high HgT_{UNF} concentrations (up to 28 pmol L^{-1}) in the beginning and the middle of dry seasons (March to April then August to November). The wet seasons (May to July then December to February) displayed the lowest values (down to 4 pmol L^{-1}). This pattern was in agreement with the fact that reduced species were concentrated in the hypolimnion of the reservoir during the dry season and were diluted in the course of the wet season (Muresan *et al*., 2008; Tab. 3). The mean flow of water leaving the reservoir averaged 180 ± 70 m^3 s^{-1} for the 2003/04 period. From the tailrace monitoring data, average $MMHg_{UNF}$ and DGM concentrations in discharged waters were estimated to 2.5 ± 1.5 and 0.4 ± 0.2 pmol L^{-1}, respectively. Hence, the exportations of HgT_{UNF}, HgT_D, $MMHg_{UNF}$ and DGM were calculated to be 16 ± 5, 9 ± 2, 3 ± 1 and 0.4 ± 0.2 kg·y^{-1} respectively.

4.2.2. The role of tributaries

Local tributaries to the USE displayed HgT_{UNF} concentrations varying from 5.0 to 19.5 pmol L^{-1} and averaging 13 ± 5 pmol L^{-1} (Tab. 2). Except for the high runoff episodes, HgT_D appeared to dominate the HgT_{UNF} partitioning (7 ± 2 pmol L^{-1}, Tab. 3). Maxima of HgT_{UNF} were measured during the wet seasons (January-February and May-June 2004). At that time, 80 % of the HgT_{UNF} (17 ± 4 pmol L^{-1}) consisted of HgT_P (14 ± 5 pmol L^{-1} i.e., 800 ± 600 pmol g^{-1}). Despite the HgT partitions (5.0 ± 0.4 vs. 4.8 ± 0.4 of $Log K_{HgT}$ respectively) and concentrations in the tributaries and the dam tailrace waters were similar, we measured marked differences in the Hg speciation. The water samples from the tributaries displayed higher concentrations of HgR_{UNF} (1.3 ± 0.7 vs. 0.5 ± 0.1 pmol L^{-1}, respectively) but lower concentrations of DGM (0.11 ± 0.09 vs. 0.4 ± 0.2 pmol L^{-1}, respectively) and MMHg in the dissolved (0.8 ± 0.5 vs. 1.6 ± 0.7 pmol L^{-1}, respectively) and the particulate (80 ± 60 vs. 150 ± 100 pmol g^{-1}, respectively) phases. The amounts of Hg transported by tributaries to the USE were 4 ± 3, 2 ± 1, 0.5 ± 0.2 and 0.03 ± 0.02 kg·y^{-1} for HgT_{UNF}, HgT_D, $MMHg_{UNF}$ and DGM, respectively. These represented 25, 20, 15 and 8 % of the dam exportations.

4.3. Water oxygenation and Hg speciation

4.3.1. The artificial oxygenation system

The role of the artificial oxygenation of waters (100 m downstream of the dam, Fig. 1) was evaluated by determining Hg speciation on both sides of the aeration system. While HgT_{UNF} and HgT_D were similar (Fig. 4; Tail. vs. Pas. stations), DGM concentrations dropped by 40 %. The total atmospheric gaseous Hg within 10 m above the aeration system peaked from the “background” levels (10 pmol m^{-}

^{3}) to up to 60 pmol m^{-3} (Muresan *et al*., 2007). These measurements suggest a notable "evasion" of volatile Hg. There was a statistically significant increase (approximately 50%) in $MMHg_D$ between Tail. and Pas. sampling stations during each survey (Tab. 3). Two paired processes might account for this observation: (i) an intense biological reduction of sulfates initiated by the sudden oxygenation of the waters expelled from the dam, and (ii) an oxidative dissolution of MMHg loaded AVS (acid volatile sulfides). Considering the first mechanism, large amounts of organic substrata (0.44 ± 0.07 mmol L^{-1} of TOC) combined with high Hg concentrations (13 ± 5 pmol L^{-1} of HgT_{UNF}) and sulfidic conditions (1.2 ± 0.8 µmol L^{-1} of ΣH_2S) depicted the tailrace as a likely zone for Hg methylation. According to Dumestre *et al*. (2001), ΣH_2S-producing and ΣH_2S-consuming bacteria are closely associated within the dam expelled waters. Cycling such as this represented a small but extremely active proportion of the microbial assemblage. Considering the second mechanism, dam expelled waters mainly originated from AVS and $MMHg_P$ enriched layer of the hypolimnion (between 8 and 15 m). Partial dissolution of the discharged particles would therefore provide high $MMHg_D$ levels into the Sinnamary Estuary. Accordingly, the MMHg log partition coefficient [logK_d(MMHg); K_d(MMHg) = $MMHg_P/MMHg_D$] decreased from 5.4 ± 0.2 to 4.7 ± 0.3 in less than 300 m.

4.3.2. Mixing with the oxygenated waters from the creeks

Reaching the USE, the Hg from the tributaries underwent rapid speciation changes through complexation and methylation mechanisms. The primary variable related to Hg speciation changes was ΣH_2S. In the tributaries, the higher concentrations of dissolved O_2 (0.16 ± 0.05 mmol L^{-1}) contributed to maintain the ΣH_2S levels low (0.5 ± 0.4 µmol L^{-1}). Accordingly, the pool of reduced ligands available for Hg complexation [as strong Hg-S compounds; e.g. Log$K$ = 36.9 for $Hg^{2+} + 2HS^- = Hg(HS)_2$] was less important in the tributaries than in the tailrace waters. It is generally accepted that strong complexing agents act to lower the reduction potential of metals (van den Berg, 1984). This was supported by increased HgR_{UNF} concentrations in the tributaries (1.3 ± 0.7 pmol L^{-1}; the inherent reduction cutoff of $SnCl_2$ is about LogK_{HgR} = 19). In the USE, HgR_{UNF} and $MMHg_D$ concentrations were higher near creeks Kerenrock, Chapeau and Venus. Therefore, HgR_{UNF}/HgT_{UNF} (%) positively correlated with $MMHg_D/HgT_D$ (%) {r^2 = 0.51; [$MMHg_D/HgT_D$ (%)] = 6.4 [HgR_{UNF}/HgT_{UNF} (%)] + 0.43} (data not shown). This indicated that the more labile HgR_{UNF} specie from the tributaries may constitute an important source for Hg complexation with ΣH_2S and subsequent MMHg production in the USE.

4.4. Total mercury transport and distribution

HgT_{UNF} and HgT_D in the USE averaged (range) 11 ± 3 (5.9 - 16.9) and 6 ± 2 (2.2 - 10.5) pmol L^{-1}, respectively (Fig. 4). Between Tail. (dam end-member) and Sin. (saline end-member) stations, HgT_D decreased from 9 ± 2 to 5 ± 2 pmol L^{-1} (i.e. from 80 to 60 % of HgT_{UNF}). USE HgT_D concentrations were highest in long dry season (9 ± 1 pmol L^{-1}) declined in the short wet and dry (orderly 5 ± 2 and 7 ± 1 pmol L^{-1}) seasons and reached a minimum in long wet season (3 ± 1 pmol L^{-1}). USE HgT_D concentrations measured in the dry seasons (8 ± 1 pmol L^{-1}) reflected the average hypolimnion of the reservoir (8 ± 2 pmol L^{-1}; Tab. 2, Section 4.2.1.). The decrease in HgT_D during the wet season (4 ± 2 pmol L^{-1}) likely resulted from the dilution of the dam outflow by downstream tributaries (5 ± 2 pmol L^{-1}) or lateral runoff waters.

High percentages of dissolved strongly complexed mercury (50 ± 10 % of the HgT_D; calculated as $Hg_{DSC} = HgT_D - HgR_D - MMHg_D$) revealed that a notable proportion of HgT_D in the USE was bound to dissolved OM (DOM) and sulfides (as these strong ligands controls the Hg speciation in solution in low oxygen zones). Colloids depict a transitional domain (from 10^{-3} to 1 µm) between which was considered dissolved (<0.45 µm) and particulate (>0.45 µm) material. In the USE, intense degradation of OM suggested that organic ligands (such as thiols) played a major role in the complexation of HgT_D (Fig. 5). Using our data, we determined the speciation of Hg_{DSC} in the presence of DOM and ΣH_2S by running the speciation code line WHAM 6. The calculations showed that the proportions of Hg_{DSC} bound to DOM were between 35 and 45 % (42 ± 4 % on average) and increased with the distance from the dam. These calculations were supported by a positive correlation between HgT_D and DOC (r^2 = 0.78). The presence of micromolar ΣH_2S pointed out an extra contribution of sulfidic ligands. Rozan et al. (2000) stated that metal-sulfide complexes (Fe-S, Zn-S and Cu-S) can persist for weeks under oxic conditions. Besides, Hsu-Kim and Sedlak (2005) observed strong Hg-S complexes in the sulfidic

effluents from municipal wastewater. Using mole ratios similar to those observed for Cu and Zn [predominantly 1:1 metal to sulfur ratio (M_3S_3) and a small quantity of compounds with a 2:3 metal to sulfur ratio (M_4S_6)], strong Hg-S complexes were calculated to have thermodynamic stability constants up to Log β = 130.4 (Hg_3S_3) and Log β = 194.7 (Hg_4S_6). In the USE, strong Hg-S complexes constituted more than 50 % of the Hg_{DSC} but their contribution decreased with the distance from the dam (from 65 down to 53 %). From the observed decrease, the average half-life of the strong Hg-S pool of complexes was estimated to be 3-7 days.

Since DOM and inorganic sulfides competed for Hg binding, we observed a "U" shape relationship between HgT_D and. ΣH_2S (Fig. 5). High ΣH_2S concentrations (> 1 µmol L^{-1}) would enhance the Hg mobilization through thermodynamic equilibrium with cinnabar ($HgS_{(s)}$): formation of Hg-S complexes in the dissolved (Morel *et al*., 1998). Low ΣH_2S concentrations (< 1 µmol L^{-1}) would induce a predominance of the oxidative dissolution processes (e.g. of AVS and Hg-S clusters) and thus enhance the Hg transfer to the DOM. Hence, around 1 µmol L^{-1} of ΣH_2S, limited formation of Hg-S complexes and Hg transfer to the DOM would correspond to a maximum for HgT_D scavenging.

Average concentrations of HgT_D in the USE were 30 % lower than the average concentrations at the Tail. station (Tab. 2). The positive correlation between FeT_D and ΣH_2S (r^2 = 0.82) suggested a dynamic equilibrium between dissolved species and iron sulfides (monosulfide/AVS and/or pyrite). Their elevated specific surface (several $m^2\ g^{-1}$) coupled with the high affinity of Hg for sulfide ligands depicted AVS as potential scavenging agents. Beyond AVS, the main pathway for HgT_D scavenging was related to Fe oxyhydroxides. The most abundant metal in solution, FeT_D decreased from 18 $\pm$ 5 to 4 $\pm$ 2 µmol L^{-1} between Tail. and Sin. stations. 30 $\pm$ 10 % of the observed decrease originated from the artificial aeration of waters *circa* 100 m downstream of the dam (Fig.2). Thus, applying the model described in Section 2.3. to the HgT_D vs. FeT_D relationship (r^2 = 0.69), we estimated that 400 $\pm$ 100 nmol of HgT_D are scavenged per mol of oxidized FeT_D (Fig. 5). As *circa* 7000 tons of FeT_D were exported from the dam annually, oxidation of Fe^{II} to Fe oxyhydroxides would have removed 10 $\pm$ 3 kg y^{-1} of Hg from the dissolved phase. This high-end estimate is lower than annual dam exportations of HgT_{UNF} (16 kg y^{-1}) but exceeded those of HgT_D (9 kg y^{-1}).

4.5. Gaseous mercury production and consumption

Between the Petit-Saut dam and Sin. station (70 km downstream), DGM decreased from 0.37 $\pm$ 0.10 to 0.14 $\pm$ 0.10 pmol L^{-1}. This corresponded to an average diminution greater than 60 % (Fig. 4). The amount of DGM transferred to the atmosphere was calculated by multiplying the annual amount of discharged water (about 6 10^9 m^3) and the overall average decrease of DGM concentrations for all surveys (0.23 $\pm$ 0.10 pmol L^{-1}). This calculation supposed that the measured DGM decrease issued only from degassing processes and that endogenous DGM production was negligible. Thus, the USE transferred 0.2 $\pm$ 0.1 kg y^{-1} of Hg^0 to the atmosphere which represented less than 2 % of the dam exported amount of HgT_{UNF} (16 kg y^{-1}). About 50 % (i.e. 0.1 kg y^{-1}) of the transferable DGM degassed when passing through the artificial aeration system.

The reduced penetrability of light (< 1 m) limited the Hg photoreduction. We thus probed the abiotic Hg^0 production by the Fe^{II} to $Fe(OH)_3$ oxidation in the presence of hematite particles: adsorption of Fe^{II} to the surface of haematite nanoparticles creates very reactive sites for the Hg^{II} reduction (Peretyazhko *et al*. 2006). Gained data showed that a maximum of DGM production (2 pmol L^{-1} h^{-1}) was concomitant to a Fe^{II} decrease in the dissolved phase (from 20 to 8 µmol L^{-1}). In the USE, between Tail. and Ven. stations, the suspended particles of hematite were visible by sight. In addition, the DGM production by Fe^{II} to $Fe(OH)_3$ oxidation was apparent by a positive correlation between DGM and FeT_D concentrations (r^2 = 0.73) (Figs. 2 and 4). We calculated that 15 $\pm$ 3 nmol of DGM are in equilibrium with every mol of FeT_D (Fig. 5). As roughly 7000 tons of FeT_D were annually discharged downstream of the dam, 0.3 $\pm$ 0.1 kg y^{-1} of DGM would have been abiotically produced. As a result, Fe driven production of DGM within the first 30 km of the USE was almost equivalent to dam exportations (0.4 $\pm$ 0.2 kg·y^{-1}, Section 4.2.1).

In the USE, DGM scavenging resulted from both direct Hg^0 oxidation and its strong complexation with POC (decrease of the Hg availability towards reduction). A negative correlation between DGM and POC (r^2 = 78) supported these mechanisms (Fig.5). The OM plays a key role in the photochemical reduction of ionic Hg^{II} to Hg^0 (Alberts *et al*., 1974; Allard and Arsenie, 1991; Nriagu, 1994) and its subsequent reoxidation (Amyot *et al*., 1997; Ravichadran, 2004; O'Driscoll *et al*., 2006). In the presence of O_2, the OM catalyzed Hg^0 reoxidation can be formulated as:

$$2CH_2O + Hg^0 + 2.5O_2 \rightarrow Hg(OH)_2 + 2CO_2 + H_2O$$

To probe this mechanism, we monitored the HgR_D production that occurred during the DGM scavenging (as DGM oxidation should produce weak Hg complexes; data not shown). We determined that 30-50 % of the scavenged DGM were oxidized as HgR. To probe the second mechanism, the complexation of DGM with POC was modeled by running the speciation code line WHAM 6. Between Tail. and Sin. sampling stations, the proportions of particulate strongly complexed Hg (calculated as $Hg_{PSC} = HgT_P – HgR_P – MMHg_P$) bound to POC increased from 22 to 27 %. Assuming that 10 ± 7 % (i.e. the average percentage of DGM/Hg_{DSC}) of Hg_{PSC} originated from DGM, we estimated that 10-30 % of the DGM scavenging results from strong complexation with POC. Overall, from the DGM vs. POC relationship, we calculated that 5 ± 1 nmol of DGM were scavenged per mol of POC in solution. Scaled to the 4 10^9 g y^{-1} POC discharged in the downstream of the dam, DGM scavenging in the USE compensated the Fe driven production of DGM (both 0.3 ± 0.1 kg y^{-1}). Eventually, the atmospheric Hg evasion resulted from (i) the dam exportations, (ii) the net balance between in situ Hg reduction and oxidation processes, and (iii) the Hg^0 complexation with POC.

In the USE, DGM negatively correlated with the log partition coefficient of HgT (r^2 = 0.45): DGM correlated positively with HgT_D (r^2 = 0.63) and negatively with HgT_P (r^2 = 0.23). Investigating the HgT_D speciation, significant negative correlations were observed between DGM and $MMHg_D$ (r^2 = 0.45; $[DGM]_{pmol\ l\text{-}1} = -0.1\ [MMHg_D]_{pmol\ L\text{-}1} + 0.35$; Fig. 6), and DGM and $MMHg_D/HgT_D$ (%) {r^2 = 0.61; [DGM]pmol L-1 = 1.1 [MMHg D/HgTD (%)]-0.6}. Observations such as these suggested either (i) a bacterial resistance to Hg through potential demethylation by the mer operon or (ii) that MMHgD production limits Hg availability with respect to reduction (Fig. 6). More unusual was the absence of significant correlation with HgRUNF (commonly considered as a precursor of DGM). The reduced light penetrability combined with high OM concentrations (0.47 mmol L-1 of TOC) and wide pool of reduced ligands (0.7 µmol L-1 of ΣH2S) may explain the lack of relationship. Hence, in this particular environment, the HgDSC may define the active fraction involved in the DGM formation process.

4.6. The methylmercury redox cycle

4.6.1. Methylmercury partition and distribution

The USE concentration of $MMHg_{UNF}$ averaged 3.7 ± 1.0 pmol L^{-1} with 2.0 ± 0.9 pmol L^{-1} as dissolved and 1.8 ± 1.2 (i.e. 220 ± 130 pmol g^{-1}) pmol L^{-1} as particulate (Tab. 2). In the dissolved phase, the methylated percentage [$MMHg_D/HgT_D$ (%)] averaged 40 ± 20 % and reached 90 % between Ker. and Bra. stations in the wet seasons. In the particulate phase, the methylated percentage [$MMHg_P/HgT_P$ (%)] averaged 40 ± 20 % and reached 97 % between Bra. and Sin. stations in the dry seasons (Figs. 4 and 6). Regarding the $\log K_d(\mathrm{MMHg})$, calculated values, averaging 5.0 ± 0.4, were in the upper range of data available from the literature (e.g., Cai *et al*., 1999; Choe and Gill, 2001). Similar log partition coefficients were found in the Trinity River (USA) for colloidal (1 kDa-0.45 µm) and truly dissolved (< 1 kDa) fractions (Choe and Gill, 2001). In the USE, $MMHg_D$ and POC displayed a significant positive relationship with seasons (r^2 = 0.61; $[MMHg_D]_{pmol\ L\text{-}1} = 180\ [POC]_{mmol\ L\text{-}1} – 8.8$; Fig. 5). Since colloids primarily consist of finer particles and organic macromolecules that pass into the filtrate, we expected that colloidal and particulate phases shared a common pool of ligands (e.g. reduced sulfur and thiol moieties). This was supported by positive correlations between (i) $MMHg_D$ and the organic component of particles (r^2 = 0.44; $[MMHg_D]_{pmol\ L\text{-}1} = 0.12\ [POC]_{mmol\ g\text{-}1} – 0.8$, Fig. 5), and (ii) log partitions coefficients of MMHg and organic C (Figs. 5 and 6). Using the WHAM 6 program, we calculated that nearly 100 % of the $MMHg_D$ in the USE was associated with colloidal OM.

$MMHg_{UNF}$ in the tributaries averaged 1.3 ± 0.6 pmol L^{-1} of which 0.8 ± 0.5 and 0.4 ± 0.3 (i.e. 80 ± 60 pmol g^{-1}) pmol L^{-1} were $MMHg_D$ and $MMHg_P$, respectively. As a result, during the wet seasons, the tributaries contributed to the USE dilution with MMHg in the vicinity of Creek Kerenrock, Creek Venus and Creek Saulnier (Fig. 4). In the tributaries, low ΣH_2S concentrations coupled with high Eh values (> 350 mV) settled unfavorable conditions for Hg methylation. However, quantifiable MMHg concentrations highlighted the existence of diffuse sources. Main sources of MMHg consisted of the sandy sediments, the leaf litter and the biofilms. While the methylation rates were low in the sediments (0.3 ± 0.2 % hr^{-1}), higher values were determined in the surface litter (1.4 ± 0.4 % hr^{-1}) and the biofilms (0.6 ± 0.2 % hr^{-1}) (Mason pers. com.). The leaf litter and the biofilms from the tributaries consisted mainly of OM at different stages of humification (> 80 % dry weight). Substrata such as these may

have built up favorable methylating conditions through the microbial activity and the oxygen depletion associated with the OM mineralization. Besides, from the 2003/04 tailrace water monitoring, an inverse relationship was observed between $MMHg_{UNF}$ and the redox ($r^2 = 0.56$; $[MMHg_{UNF}]_{pmol\ L\text{-}1} = -0.03\ Eh_{mV} + 8.3$). Hence, reductive conditions not only promote Hg methylation in the USE but also accompany the increase of $MMHg_{UNF}$ in the waters exported from the dam (Fig. 3). Thus, in wet seasons, we propose the occurrence of two opposite processes: (i) elevated $MMHg_{UNF}$ exportations via the dam tailrace (up to 0.15 mol d^{-1}) and (ii) localized dilution of concentrations by creeks inflows (above 80 $m^3\ s^{-1}$).

4.6.2. In situ methylmercury production

A preliminary budget can be built up for MMHg in the USE using the measurements in the main water sources. The most striking conclusion concerning the 2003-2005 period was that USE exported 5.5 $\pm$ 0.7 kg y^{-1} $MMHg_{UNF}$ (55% as $MMHg_D$) while barely 3 $\pm$ 1 and 0.5 $\pm$ 0.2 kg y^{-1} $MMHg_{UNF}$ (50 and 70 % as $MMHg_D$) reach the USE via the Petit-Saut dam and the river-tributaries, respectively. Hence, in the USE, the average Hg methylation rate [calculated as the ratio of the annual produced amount of $MMHg_{UNF}$ (2 kg) and the reservoir exports of unmethylated Hg (13 kg)] was 0.3-0.7 % hr^{-1}. Despite uncertainties surrounding these figures, there is a strong suggestion that a large quantity of MMHg was produced in the USE itself.

Micromolar ΣH_2S concentrations (0.7 $\pm$ 0.5 µmol L^{-1}) and a reasonable balance between O_2 and $MMHg_D$ levels ($r^2 = 0.47$; $[MMHg_D]_{pmol\ L\text{-}1} = 15\ [O_2]_{mmol\ L\text{-}1}$) supported the USE in situ Hg methylation (Fig. 6). The role of O_2 was dual. On the one hand, water oxygenation favors the ΣH_2S oxidation to SO_4 (SRB substratum). Between Tail. and Ven. sampling stations, SO_4 increased from 6 to 16 µmol L^{-1} while ΣH_2S decreased ($r^2 = 0.55$; $[SO_4]_{\mu mol\ L\text{-}1} = -3\ [\Sigma H_2S]_{\mu mol\ L\text{-}1} + 14$). On the other hand, an excess of oxygenation inhibits the SRB activity to the benefits of oxygen metabolizing bacteria (e.g., Fe^{II}, ΣH_2S, CH_4, oxidizers; Dumestre *et al*., 2001). The O_2 levels up to saturation (%) and the $MMHg_D/HgT_D$ (%) (a proxy of the local production of $MMHg_D$, Benoit *et al*., 2001, 2003) displayed an inverse evolution [$r^2 = 0.37$; $MMHg_D/HgT_D$ (%) = -1.2 O_2 (%) + 100]. Hence, low O_2 depicted the sites of moderate $MMHg_D$ concentrations but intense endogenous Hg methylation (such as Deg. station).

The hypothesis of in situ Hg methylation emerged from: (i) the rapid increase of $MMHg_{UNF}$ and $MMHg_D$ concentrations between Tail. and Pas. stations (Tab. 3 and Fig. 4) and (ii) the parallel study of ΣH_2S concentrations and $MMHg_D/HgT_D$ (%) in the USE. On the one hand, between Tail. and Pas. stations, the average Hg methylation rate [calculated as the ratio of the annual produced amount of $MMHg_{UNF}$ (approximately 1 kg) and the reservoir export of unmethylated Hg (13 kg)] was 10-15 % hr^{-1} and reached 27 % hr^{-1} in the dissolved phase. Comparatively, the rate of MMHg release due to the oxidative dissolution of AVS [calculated from the measured decrease of $MMHg_P$, of 100 $\pm$ 70 pmol g^{-1}] averaged 9 $\pm$ 5 % hr^{-1} (i.e. 0.6 $\pm$ 3 kg yr^{-1}). This represented 90 $\pm$ 30 % of the observed $MMHg_D$ produced in the immediate vicinity of the artificial aeration system and 50 $\pm$ 30 % of the $MMHg_D$ produced in the USE. On the other hand, in the downstream of the Pas. station, the bulge shape of the $MMHg_D/HgT_D$ (%) vs. ΣH_2S relationship suggested an optimum ΣH_2S concentration for Hg methylation (Fig. 6). The sites of low and intermediate ΣH_2S concentrations (< 1 µmol L^{-1}) exhibited analogous variations of both parameters {$r^2 = 0.70$; $MMHg_D/HgT_D$ (%) = 100 $[\Sigma H_2S]_{\mu mol\ L\text{-}1}$ + 10}. This was consistent with the hypothesis of neutral Hg-S complexes controlling the bioavailability of inorganic mercury towards SRB (Benoit *et al*., 1999, 2003). On the contrary, more sulfidic environments (> 1 µmol L^{-1}) exhibited inverse variations between $MMHg_D/HgT_D$ (%) and ΣH_2S concentrations {$r^2 = 0.76$; $MMHg_D/HgT_D$ (%) = -50 $[\Sigma H_2S]_{\mu mol\ L\text{-}1}$ + 120} (Fig. 6). This would account for a lessening in Hg bioavailability due to formation of ionic Hg-S complexes [$HgS(SH)^-$, HgS_2^{2-} etc.] and/or precipitation of inorganic Hg as cinnabar. A balance between water oxygenation which controls SRB activity through production of sulfates and ΣH_2S level that governs Hg bioavailability played a large role in the local production of MMHg.

Lowering pH contributed to decrease the log partition coefficient of HgT [$r^2 = 0.33$; $\log K_d(HgT) = 0.5\ pH + 2.0$] and increase that of MMHg [$r^2 = 0.46$; $\log K_d(MMHg) = -0.9\ pH + 10.0$] (Fig. 6). On the one hand, water acidification would promote the HgT_P mobilization towards the dissolved phase (e.g. via acidic dissolution of AVS and/or Fe oxyhydroxides). On the other hand, according to the Benoit *et al*. (2003) formulation:

$$RSHg^+ + H_2O + HS^- = HgS^0 + RSH + H^+$$

increasing $[H^+]$ leads to decreasing $[HS^-]$, and as a result, HgS^0 (the hypothetical substratum of methylation) will decrease relative to $RSHg^+$ i.e., methylation rate and $MMHg_D$ should at length decrease. This consideration was supported by a positive correlation between pH and $MMHg_D/HgT_D$ (%) [r^2 = 0.42; $MMHg_D/HgT_D$ (%) = 60 pH – 300]. Hence, a reasonable balance between the Hg mobilization from the particulate phase (which increases with $[H^+]$) and the HgS^0 production in the dissolved phase (which decreases with $[H^+]$) also determined the production of MMHg. In conclusion, slightly acidic waters, as in the USE, provide favorable conditions for MMHg production.

4.6.3. Methylmercury trapping and mobilization

According to Benoit *et al*. (2003), the complexation of MMHg to OM or inorganic sulfide phases are comparable since both involve interactions with thiols or other reduced S species. The same authors proposed that lowering pH would favor the MMHg association with particles:

$$RS\text{-}H + CH_3Hg(OH) = RS\text{-}HgCH_3 + H_2O$$

This was testified with our data: $MMHg_P$ concentrations increased with decreasing pH (r^2 = 0.61; $[MMHg_P]_{pmol\ g\text{-}1}$ = -280 pH + 1800). A marked inverse relationship (r^2 = 0.60, Fig. 6) was also observed between $MMHg_P/HgT_P$ (%) and $MMHg_D/HgT_D$ (%). We thus concluded to a high mobility of methylated Hg species between the dissolved and particulate phases along the USE. Acid-base mechanisms and ΣH_2S levels seemingly drove the MMHg phase changes. Maxima of $MMHg_P/HgT_P$ (%) corresponded to the most acidic and oxidized waters (such as Ker. or Ven. stations) whereas slightly acidic and sulfidic milieus displayed among highest $MMHg_D/HgT_D$ (%) (like Pas. or Deg. stations). Overall, changes in MMHg binding resulted in a 5 % increase of $MMHg_P/HgT_P$ (%) per 0.1 pH unit of water acidification.

Trapping of $MMHg_D$ and mobilization of $MMHg_P$ constituted dynamic processes that occurred simultaneously in the Sinnamary Estuary. To illustrate (Fig. 5), below 10 µmol L^{-1}, the distributions of FeT_D and $MMHg_D$ correlated positively (r^2 = 0.65; $[MMHg_D]_{pmol\ L\text{-}1}$ = 0.24 $[FeT_D]_{\mu mol\ L\text{-}1}$ + 0.73). Conversely, above that limit, FeT_D and $MMHg_D$ correlated negatively (r^2 = 0.54; $[MMHg_D]_{pmol\ L\text{-}1}$ = -0.12 $[FeT_D]_{\mu mol\ L\text{-}1}$ + 4.2). An inverted pattern was observed when plotting the FeT_D vs. $MMHg_P$. Thus, $MMHg_P$ mobilization (e.g. AVS dissolution) dominated in the vicinity of the Petit-Saut dam while $MMHg_D$ trapping (e.g. precipitation of Fe oxyhydroxides) prevailed further along the way to the Atlantic Ocean. Applying the model described in Section 2.3. to $MMHg_D$ and $MMHg_P$ vs. FeT_D relationships, we calculated that (i) 130 $\pm$ 30 nmol of $MMHg_P$ are mobilized per mol of discharged FeT_D and (ii) nearly 250 $\pm$ 50 nmol of $MMHg_D$ are scavenged per mol of oxidized FeT_D. Scaled to the 7000 tons of FeT_D discharged downstream of the dam, 3.0 $\pm$ 0.7 kg y^{-1} of $MMHg_P$ were transferred to the dissolved phase while close to 4.9 $\pm$ 0.9 kg y^{-1} were subsequently scavenged on authigenic particles. If we assume that the excess of scavenging (close to 1.9 kg) originated mainly from in situ methylation processes, then at least 30-50 % of the downstream $MMHg_{UNF}$ amount (5.5 $\pm$ 0.7 kg) was endogenically produced.

5. Concluding Remarks

This is the first investigation of the methylation potential of a tropical estuary that undergoes hypolimnetic discharges was probed. Extensive field measurements of Hg partitioning and speciation as well as long-term concentration monitoring of the dissolved and particulate phases of the Sinnamary Estuary indicated that methylation conformed to Benoit's neutral complex theory. Accordingly, the balance between sulfides concentration, which governs Hg bioavailability, and water oxygenation, which controls SRB activity through production of sulfates, determines which stations have high $MMHg_D$ concentrations. Besides, acid-base mechanisms, along with Fe cycling, had a significant impact on MMHg partitioning between phases.

To conclude, the Sinnamary Estuary constituted a chemical reactor with respect to Hg methylation and reduction. Atmospheric Hg evasion reflected (i) the DGM export from the dam, (ii) the net balance between the reduction and the oxidation processes and (iii) the Hg^0 complexation with POC. Hence, the USE production of MMHg exceeded the amount of Hg transferred to the atmosphere by one order of magnitude: 2.0 $\pm$ 1.5 and 0.2 $\pm$ 0.1 kg y^{-1}, respectively.

Acknowledgements

We acknowledge Y. Dominique for his suggestions and technical assistance during in situ campaigns and laboratory tasks. We also thank B. Burban, C. Reynouard, P. Cerdan, V. Horeau, R. Aboïkoni, L. Guillemet and R. Vigouroux for their participation and facilitation to sampling and analyses. This work has been financially supported by CNRS (Conseil National de la Recherche Scientifique) and EDF (Electricité de France) grant N° F01381/0.B. This manuscript also benefited from thorough reviews by three anonymous reviewers.

References

Alberts J. J., Schindler J. E., Miller R. W. and Nutter D. E. (1974) Elemental mercury evolution mediated by humic acid. *Science* 184, 895-897.

ALLARD B. and ARSENIE L. (1991) Abiotic reduction of mercury by humic substances in aquatic system. An important process for the mercury cycle. *Water Air Soil Pollut.* 56, 457-464.

AMOUROUX J. M. (2003) Genèse et devenir des mangroves. L'exemple de la Guyane. Cycles de conférences 2002 / 2003-Perspectives: Quel avenir pour l'Homme?

Amyot M., Mierle G., Lean D. and McQueen D. J. (1997) Effect of solar radiation on the formation of dissolved gaseous mercury in temperate lakes. *Geochim. Cosmochim. Acta* 61, 975-987.

BAEYENS W. and LEERMAKERS M. (1998) Elemental mercury concentrations and formation rates in the Scheldt estuary and the North Sea. *Mar. Chem.* 60, 257-266

BECKETT R. and. LE N. P. (1990) The role or organic matter and ionic composition in determining the surface charge of suspended particles in natural waters*. Colloid. Surface.* 44, 35-49.

BENOIT J. M., GILMOUR C. C., HEYES A., MASON R. P. and MILLER C. L. (2003) Geochemical and biological controls over mercury production and degradation in aquatic systems*. ACS Sym. Ser.* 835, 262-297.

BENOIT J. M., MASON R. P., GILMOUR C. C. and AIKEN G. R. (2001) Constants for mercury binding by dissolved organic matter isolates from the Florida Everglades. *Geochim. Cosmochim. Acta* 65, 4445-4451.

BENOIT J. M., GILMOUR C. C., MASON R. P. and HEYES A. (1999) Sulfide Controls on Mercury Speciation and Bioavailability to Methylating Bacteria in Sediment Pore Waters. *Environ. Sci. Technol.* 33,. 951-957.

BENOIT J. M., GILMOUR C. C., MASON R. P., RIEDEL G. S. and RIEDEL G. F. (1998) Behavior of mercury in the Patuxent River estuary. *Biogeochem*. 40, 249-265.

BISINOTI M. C. and JARDIM W. F. (2005) Production of organic mercury from Hg^0: experiments using microcosms*. J. Braz. Chem. Soc*. 14, 244-248.

BLOOM N. S. and EFFLER S. W. (1990) Seasonal variability in the mercury speciation of Onondaga Lake (New York). *Water Air Soil Pollut.* 53, 25-265.

BLOOM N. S. (1989) Determination of picogram levels of methylmercury by aqueous phase ethylation followed by cryogenic gas chromatography with cold vapour atomic fluorescence detection. *Can. J. Fish. Aquat. Sci.* 46, 1131-1140.

BLOOM N. S. and FITZGERALD W. F. (1988) Determination of volatile mercury species at the picogram level by low-temperature gas chromatography with cold-vapour atomic fluorescence detection. *Anal. Chim. Acta* 208, 151-161.

Boughriet A., Ouddane B., Fischer J. C., Wartel M. and Leman G. (1992) Variability of dissolved Mn and Zn in the Seine estuary and chemical speciation of these metals in suspended matter. *Water Res.* 26, 1359-1378.

Boyle E. A., Edmond J. M. and Sholkovitz E. R. (1977) The mechanism or iron removal in estuaries. *Geochim. Cosmochim. Acta*, 41, 1313-132.

BUFFLE J. (1988) Complexation reactions in aquatic systems, Ellis Horwood Ltd.

CAI Y., JAFFÉ R. I. and JONES R. D. (1999) Interactions between dissolved organic carbon and mercury species in surface waters of the Florida Everglades*. App. Geochem.* 14, 395-407.

CHOE K-Y. and GILL G. A. (2001) Isolation of colloidal monomethyl mercury in natural waters using cross-flow ultrafiltration techniques. *Mar. Chem.* 76, 305-318.
CHOI S. C., CHASE T. J. and BARTHA R. (1994) Metabolic pathways leading to mercury methylation in Desulfovibrio desulfuricans LS. *Appl. Environ. Microbiol.* 60, 4072–4077.
COMPEAU G. and BARTHA R. (1985) Sulfate reducing bacteria: principal methylators of Hg in anoxic estuarine sediments. *Appl. Environ. Microbiol*. 50, 498-502.
COMPEAU G. and BARTHA R. (1984) Methylation and demethylation of mercury under controlled redox, pH and salinity conditions. *Appl. Environ. Microbiol.* 48, 1203-1207.
COQUERY M., COSSA D. and SANJUAN J. (1997) Speciation and sorption of mercury in two macro-tidal estuaries. *Mar. Chem.* 58, 213-227.
COSSA D., AVERTY B., BRETAUDEAU J. and SENARD A. S., (2003) Spéciation du mercure dissous dans les eaux marines. *Méthodes d'analyse en milieu marin*, Editions Ifremer 27 pp.; ISBN 2-84433-125-4.
COSSA D., COQUERY M., NAKHLE K. and CLAISSE D. (2002) Dosage du mercure total et du monomethylmercure dans les organismes et les sédiments marins. *Méthodes d'analyse en milieu marin*, Editions Ifremer 27pp.; ISBN 2-84433-105-X.
COSSA D. and GOBEIL C. (2000) Mercury speciation in the lower St. Lawrence estuary. *Can. J. Fish. Aquat. Sci.* 57, 138-147.
COSSA D. and GOBEIL C. (1996) Speciation and mass balance of mercury in the lower Saint Laurent estuary and Saguenay Fjord (Canada). *4th International Conference on Mercury as a Global Pollutant* Book of Abstracts, Hamburg 458, 4-8.
DE JUNET A. (2004) Etude qualitative de la matière organique particulaire dans le réservoir de Petit-Saut (Guyane Française) : Composition Isotopique ($\delta^{13}C$), élémentaire (C/N) et pigmentaire. *Master report*, Talence, 41 pp.
DUMESTRE J-F., EMILIO C. O., RAMON M. and PEDROS-ALIO C. (2001) Changes in bacterial assemblages in a equatorial river induced by water eutrophication of Petit Saut dam reservoir (French Guiana). *Aquat. Microb. Ecol.* 26, 209-221.
DYRSSEN D. and WEDBORG M. (1991) The sulphur–mercury(II) system in natural waters. *Water Air Soil Pollut*. 56, 507-519.
DZOMBAK D. A. and MOREL F. M. M. (1990) Surface complexation modeling Hydrous ferric oxide. New York John Wiley and Sons, 393 pp.
GILMOUR C. C., HENRY E. A. and MITCHELL R. (1992) Sulfate Stimulation of Mercury Methylation in Freshwater Sediments. *Environ. Sci. Technol.* 26, 2281-2287.
Goulet R. R., Holmes J., Page B., Poissant L., Siciliano S. D., Lean D. R. S., Wang F., Amyot M. and Tessier A. (2007) Mercury transformations and fluxes in sediments of a riverine wetland. *Geochim. Cosmochim. Acta* 71, 3393-3406.
GUIMARAES J. R. D., ROULET M., LUCOTTE M. and MERGLER, D. (2000a) Mercury methylation along a lake-forest transect in the Tapajós river floodplain, Brazilian Amazon: seasonal and vertical variations. *Sci. Total Environ.* 261, 91-98.
GUIMARAES J. R. D., MEILI M., HYLANDER L. D., SILVA E., ROULET M., MAURO J. B. N. and LEMOS R. A. (2000b) Mercury net methylation in five tropical flood plain regions of Brazil: high in the root zone of floating macrophyte mats but low in surface sediments and flooded soils. *Sci. Total Environ.* 261, 99-107.
Heyes A., Mason R. P., Kim E. H. and Sunderland E. (2006) Mercury methylation in estuaries: Insights from using measuring rates using stable mercury isotopes. *Mar. Chem*. 102, 134-147.
HOREAU V., RICHARD S. and CERDAN P. (1998) La qualité de l'eau et son incidence sur la biodiversité. L'exemple de la retenue de Petit Saut (Guyane française). JATBA, *Rev. Ethnobiol.* 40, 53-77.
Hsu-Kim H. and Sedlak D. L. (2005) Similarities between inorganic sulfide and the strong Hg(II)-complexing ligands in municipal wastewater effluent. Environ. Sci. Technol. 39, 4035-4041.
HYDRECO: Laboratory for biological and chemical monitoring and analysis on the Petit-Saut reservoir. http://hydreco.mediasfrance.org/hydreco/
International Commission on Large Dams (2003) World register of dams 2003. Paris, France: ICOLD
JACOBS L. A., KLEIN S. M. and HENRY E. A. (1995) Mercury cycling in the water column of a seasonally anoxic urban lake (Onondaga Lake, NY). *Water Air Soil Pollut.* 80, 1-4.
JENSEN S. and JERNELOV A. (1969) Biological methylation of mercury in aquatic organisms. *Nature* 223, 753-754.
KING J. K., SAUNDERS F. M., LEE R. F. and JAHNKE R. A. (1999) Coupling mercury methylation rates to sulfate reduction rates in marine sediments. *Environ. Toxicol. Chem.* 18, 1362-1369.

Leermakers M., Galetti S., de Galan S., Brion N. and Baeyens W. (2001) Mercury in the Souther North Sea and Sheldt Estuary. *Mar. Chem.* 75, 229-248.
Liang L., Horvat M. and Bloom N. S. (1994) An improved speciation method for mercury by GC/CVAFS after aqueous phase ethylation and room temperature precollection. *Talanta* 41, 371-379.
Mantoura R. F. C., Dickson A. and Riley J. P. (1978) The complexation of metals with humic materials in natural waters. *Estuar. Coast. Mar. Sci.* 6, 387-408.
Mason R. P., Lawson N. M.,Lawrence A. L., Leaner J. J., Lee J. G. and Sheu G. -R. (1999) Mercury in the Chesapeake Bay. *Mar. Chem.* 65, 77-96.
MASON R. P., FITZGERALD W. F., HURLEY J., HANSON A. K., DONAGHAY P. L. AND SIEBURTH J. M. (1993) Mercury biogeochemical cycling in a stratified estuary. *Limnol. Oceanogr.* 38, 1227-1241.
MERCK: Photometry and test kits (2001) Certificates of quality of Spectroquant® test kits. http://www.merck.de/servlet/PB/menu/1169840/index.html
MOREL F. M. M., KRAEPIEL A. M. L. and AMYOT M. (1998) The chemical cycle and bioacculumation of mercury. *Annu. Rev. Ecol. Syst.* 29, 543-566.
Mota A. M., Cruz P., Vilhena C. and GonCalves M.L.S. (2005) Influence of the sediment on lead speciation in the Tagus estuary. *Water Res.* 39, 1451-1460.
MURESAN B., COSSA D., RICHARD S. and DOMINQUE Y. (2008) Mercury Cycling in a Tropical Artificial Reservoir: Monomethylmercury Production and Sources. *App. Geochem.* 23, 1101-1126.
Muresan B., Cossa D., Richard S., and Burbant B. (2007) Mercury speciation and exchanges at the air-water interface of a tropical artificial reservoir, French Guiana. *Sci. Total Environ.* 385, 132-145.
National Institute of Standards and Technology (2004) Critical stability constants of metal complexes database. NIST Standard Reference Database 46, U.S. Dept. Commerce, National Institute of Standard and Technology.
NRIAGU J. O. (1994) Mechanistic steps in the photoreduction of mercury in natural waters. *Sci. Total Environ.* 154, 1-8.
O'DRISCOLL N. J., SICILIANO S. D., PEAK D., CARIGNAN R. and LEAN D. R. S. (2006) The influence of forestry activity on the structure of dissolved organic matter in lakes: Implications for mercury photoreactions. *Sci. Total Environ.* 366, 880-893.
Parker J. L. and Bloom N. S. (2005) Preservation and storage techniques for low-level aqueous mercury speciation. *Sci. Total Environ.* 337, 253-263.
PARKS J. W., LUTZ A. and SUTTON J. A. (1989) Water column methylmercury in the Wabigoon/English River–Lake system: factors controlling concentrations, speciation, and net production. *Can. J. Fish. Aquat. Sci.* 46, 2184-2202.
PERETYAZHKO T., CHARLET L., MURESAN B., KAZIMIROV V. and COSSA D. (2006) Formation of dissolved gaseous mercury in a tropical lake (Petit-Saut reservoir, French Guiana). *Sci. Total Environ.* 364, 260-271.
Powell K. J., Brown P. L., Byrne R. H., Gajda T., Hefter G., Sjöberg S. and Wanner H. (2005) Chemical speciation of environmentally significant heavy metals with inorganic ligands. Part 1: the Hg^{2+}-Cl^-, OH^-, CO_3^{2-}, SO_4^{2-}, PO_4^{3-} aqueous systems, *Pure Appl. Chem.* 77, 739-800.
Ravichadran m. (2004) Interactions between mercury and dissolved organic matter – a review. *Chemosphere* 55, 319-331.
RICHARD S., ARNOUX A. and CERDAN P. (1997) Evolution in physico-chemical water quality in the reservoir and downstream following the filling of Petit-Saut dam (French Guiana). *Hydroecol. Appl.* 9 (1/2), 57-83.
RODRIGUEZ R. C. M-D., TESSIER E., AMOUROUX D., GUYONEAUD R., DURAN R., CAUMETTE P. and DONARD O. F. X. (2004) Mercury methylation/demethylation and volatilization pathways in estuarine sediment slurries using species-specific enriched stable isotopes. *Mar. Chem.* 90, 107-123.
ROULET M., LUCOTTE M. and GUIMARAES J. R. D., (2000) Methylmercury in the water, seston and epiphyton of an Amazonian river and its floodplain, Tapajos river, Brazil. *Sci. Total Environ.* 261, 43-59.
ROULET M., LUCOTTE M., CANUEL R., RHEAULT I., TRAN S. *et al*., (1998a) Distribution and partition of total mercury in waters of the Tapajós River Basin, Brazilian Amazon. *Sci. Total Environ.* 213, 203-211.
Rozan T. F., Lassman M. E., Ridge D. P. and Luther G. W. III (2000) Evidence for iron, copper and zinc complexation as multinuclear sulphide clusters in oxic rivers. *Nature.* 406, 879-8826.
SERGIO A. C-S., GUIMARAES J. R. D., MAURO J. B. N., MIRANDA M. R. and AZEVEDO M. F. O. S. (2006) Mercury methylation and bacterial activity associated to tropical phytoplankton *Sci. Total Environ.* 364, 188-199.
Sholkovitz E. R., Boyle E. A. and Price N. B. (1978) The removal of dissolved humic acids and iron during estuarine mixing. *Earth and Planet. Sc. Lett.* 40, 130-136.

Stoichev T., Amouroux D., Monperrus M., Point D., Tessier E., Bareille G., and Donard O. F. X. (2006) Mercury in surface waters of a macrotidal urban estuary (River Adour, south-west France). *Chem. Ecol.* 22, 137-148.
STUMM W., KUMMERT R. and SIGG L. (1980) A ligand exchange model for the adsorption of inorganic and organic ligands at hydrous oxide interfaces. *Croat. Chem. Acta* 53, 291-312.
Sunderland E. M., Gobas F. A. P. C., Heyes A., Branfireun B. A., Bayerd A. K., Cranstone R. E. and Parsonse M. B. (2004) Speciation and bioavailability of mercury in well-mixed estuarine sediments. *Mar. Chem.* 90, 91-105.
Tipping E. (2007) Modelling the interactions of Hg(II) and methylmercury with humic substances using WHAM/Model VI. *App. Geochem*. 22, 1624-1635.
Tipping E. (2002) Cation Binding by Humic Substances, Cambridge University Press.
Van den Berg C. M. G. (1984) Determination of the complexing capacity and conditional stability constants of complexes of copper with natural organic ligands in seawater by cathodic stripping voltammetry of copper-catechol complex ions. *Mar.Chem.* 15, 1-18.
WATRAS, C. J., BLOOM N. S., HUDSON R. J. M., GHERINI S., MUNSON R., CLAAS S. A., MORRISON K. A., HURLEY J. P., WIENER J. G., FITZGERALD W. F., MASON R. P., VANDAL G., POWELL D., RADA R., RISLOVE L., WINFREY M., ELDER J., KRABBENHOFT D. P., ANDREN A. W., BABIARZ C., PORCELLA D. B. and HUCKABEE J. W. (1994) Sources and fates of mercury and methylmercury in Wisconsin lakes. *Mercury as a Global Pollutant:* Integration and Synthesis, 153-177.
WESTALL J. C. (1987) Adsorption mechanisms in aquatic surface chemistry. *Aquatic surface chemistry:* chemical processes at the particle-water interface, 3-32.
Whalin L., Kim E.-H. and Mason R. P. (2007) Factors influencing the oxidation, reduction, methylation and demethylation of mercury species in coastal waters. *Mar. Chem.* 107, 278-294.
World Commission on Dams (2000) Dams and development; a new framework for decision-making. *Earthscan Publications Ltd*, London and Sterling, VA

Tables

CAMPAIGN	PERIOD	SEASON	SAMPLING STATION	ANALYSES
MATOUTOU 1	03-04/2003	Short dry	Tailrace, USE	Ancillary parameters: pH, Eh, O_2, POC, DOC, SO_4, ΣH_2S, FeT_D. Mercury compounds: HgT, HgR, DGM, MMHg.
MATOUTOU 2	01-02/2004	Short wet	Tailrace, USE, tributaries	
MATOUTOU 3	05-06/2004	Long wet	Tailrace, USE, tributaries	
MATOUTOU 4	11-12/2004	Long dry	Tailrace, USE, tributaries	
MATOUTOU 5	02-03/2005	Short dry	Tailrace, USE, tributaries	

Tab. 1. Summary of the different periods and sampling sites associated to the Matoutou campaigns. The Upper Sinnamary Estuary (USE) covers the given in the last column.

COMPOUND STATION	HgT_{UNF} (pmol L^{-1})	HgT_D (pmol L^{-1})	HgT_P (pmol g^{-1})	$MMHg_{UNF}$ (pmol L^{-1})	$MMHg_D$ (pmol L^{-1})	$MMHg_P$ (pmol g^{-1})	DGM (pmol L^{-1})	HgR_{UNF} (pmol L^{-1})
Reservoir hypolimnion	13 ± 6 (43) [4.0 - 25.0]	8 ± 4 (43) [1.0 - 19.4]	1300 ± 950 (37) [40 - 5290]	2.2 ± 1.0* (43) [0.35 - 8.36]	0.9 ± 0.5 (43) [0.06 - 5.88]	170 ± 90 (43) [15 - 840]	0.2 ± 0.2 (43) [0.07 - 0.74]	0.4 ± 0.3 (20) [<0.01 - 0.9]
Dam tailrace	13 ± 5 (88) [3.7 - 27.9]	8 ± 2 (27) [0.5 - 10.7]	800 ± 700 (27) [32 - 3310]	2.5 ± 1.5 (27) [0.30 - 8.40]	1.6 ± 0.7 (27) [0.11 - 2.94]	150 ± 100 (27) [27 - 320]	0.4 ± 0.2 (50) [0.06 - 0.95]	0.5 ± 0.1 (50) [0.3 – 0.8]
USE	11 ± 3 (40) [5.9 - 16.9]	6 ± 2 (40) [2.2 - 10.5]	600 ± 200 (40) [200 - 2500]	3.7 ± 1.0* (40) [1.77 - 5.54]	2.0 ± 0.9 (40) [0.24 - 4.47]	220 ± 130 (40) [59 - 590]	0.16 ± 0.08 (40) [0.04 - 0.49]	0.5 ± 0.2 (40) [0.2 - 0.9]
Tributaries	13 ± 5 (7) [5.0 - 19.5]	7 ± 2 (12) [3.1 - 10.9]	750 ± 500 (7) [290 - 1700]	1 .3 ± 0.6* (7) [0.75 - 2.38]	0.8 ± 0.5 (12) [0.29 - 2.10]	80 ± 60 (7) [17 - 240]	0.11 ± 0.09 (7) [0.02 - 0.28]	1.3 ± 0.7 (7) [0.5 - 2.3]

Tab. 2. Summary statistics for mercury concentrations: total mercury (HgT_{UNF}, HgT_D, HgT_P), monomethylmercury ($MMHg_{UNF}$, $MMHg_D$, $MMHg_P$), dissolved gaseous mercury (DGM) and reactive mercury (HgR) in various compartments that constitute the Petit-Saut reservoir / USE continuum; average ± standard deviation, (n) number of determinations, range (minimum-maximum) in box brackets. Subscript D and P refer to dissolved and particulate phases respectively; subscript UNF corresponds to unfiltered samples, except data with an asterisk which are calculated from $MMHg_D$, $MMHg_P$ and SPM

SEASONS	HgT_D (pmol L^{-1})			$MMHg_D$ (pmol L^{-1})		
	Tributaries	Dam tailrace	Pass. station	Tributaries	Dam tailrace	Pass. station
Short dry	7 ± 2 (4)	10 ± 2 (5)	10 ± 2 (5)	1.5 ± 0.4 (4)	2.0 ± 0.3 (5)	3.1 ± 0.5 (5)
Long dry	8 ± 2 (3)	11 ± 2 (3)	10.2	1.4 ± 0.5 (3)	2.3 ± 0.4 (3)	4.47
Short wet	3 ± 1 (2)	9 ± 2 (5)	9.2	0.4 ± 0.2 (2)	0.7 ± 0.2 (5)	2.44
Long wet	6 ± 3 (3)	6 ± 1 (5)	3.6	0.7 ± 0.1 (3)	1.4 ± 0.2 (5)	2.05

Tab. 3. Seasonal variability of dissolved total (HgT_D) and monomethyl ($MMHg_D$) mercury in the principal freshwater inputs to the USE (Creek-tributaries vs Dam tailrace). Effect of the artificial aeration system on HgT_D and $MMHg_D$ levels (Dam tailrace *vs* Pass. station).

Figures

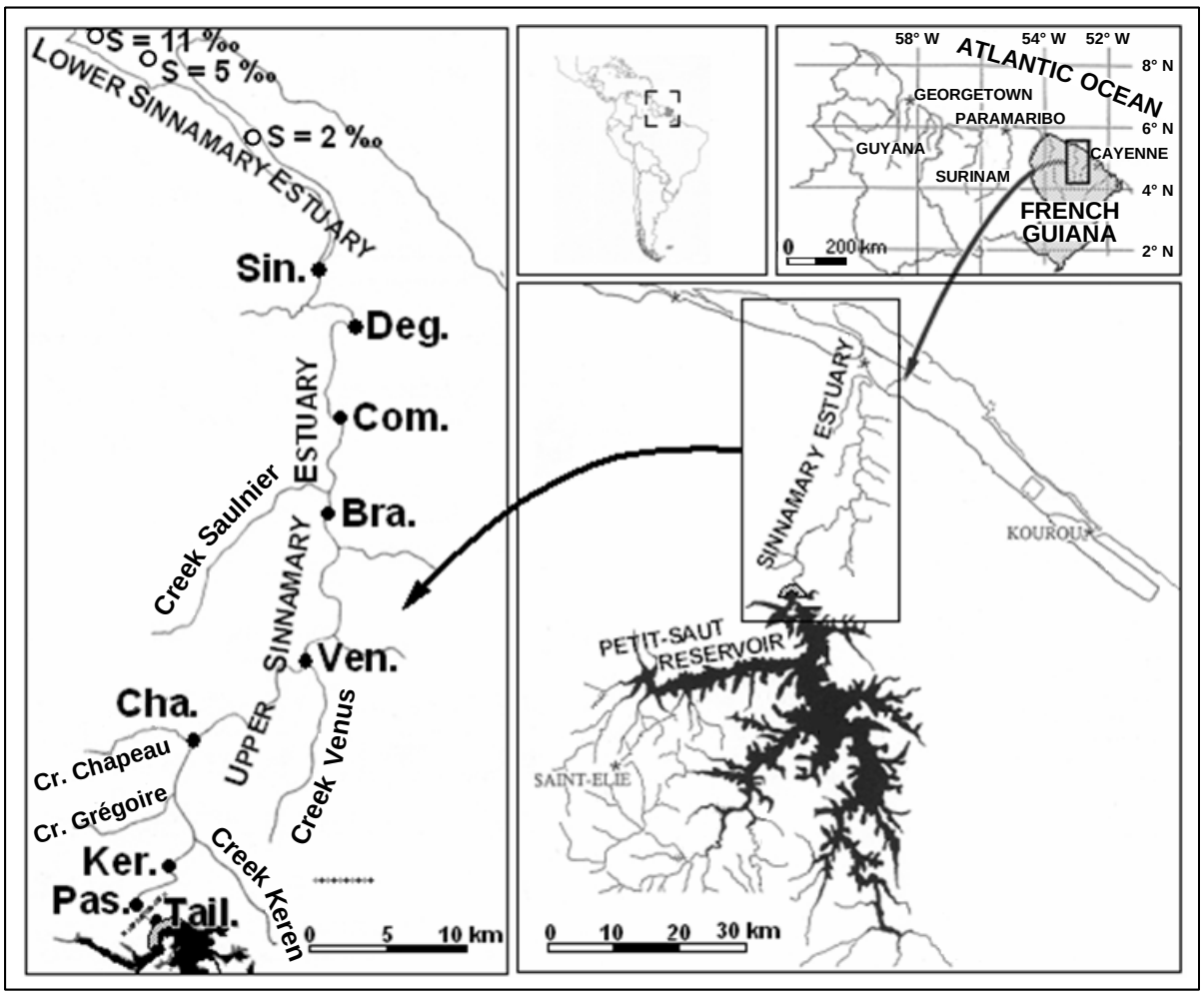

Fig. 1. The Sinnamary Estuary study area. Filled circles were sampled during Matoutou 1, 2, 3, 4 and 5 campaigns. The Kerenrock, Gregoire, Chapeau, Venus and Saulnier creek-tributaries to the USE were sampled during the Matoutou 2,3,4,5 sampling campaigns. The dam discharged waters were monitored (between March 2003 and December 2004) at the Tail. station.

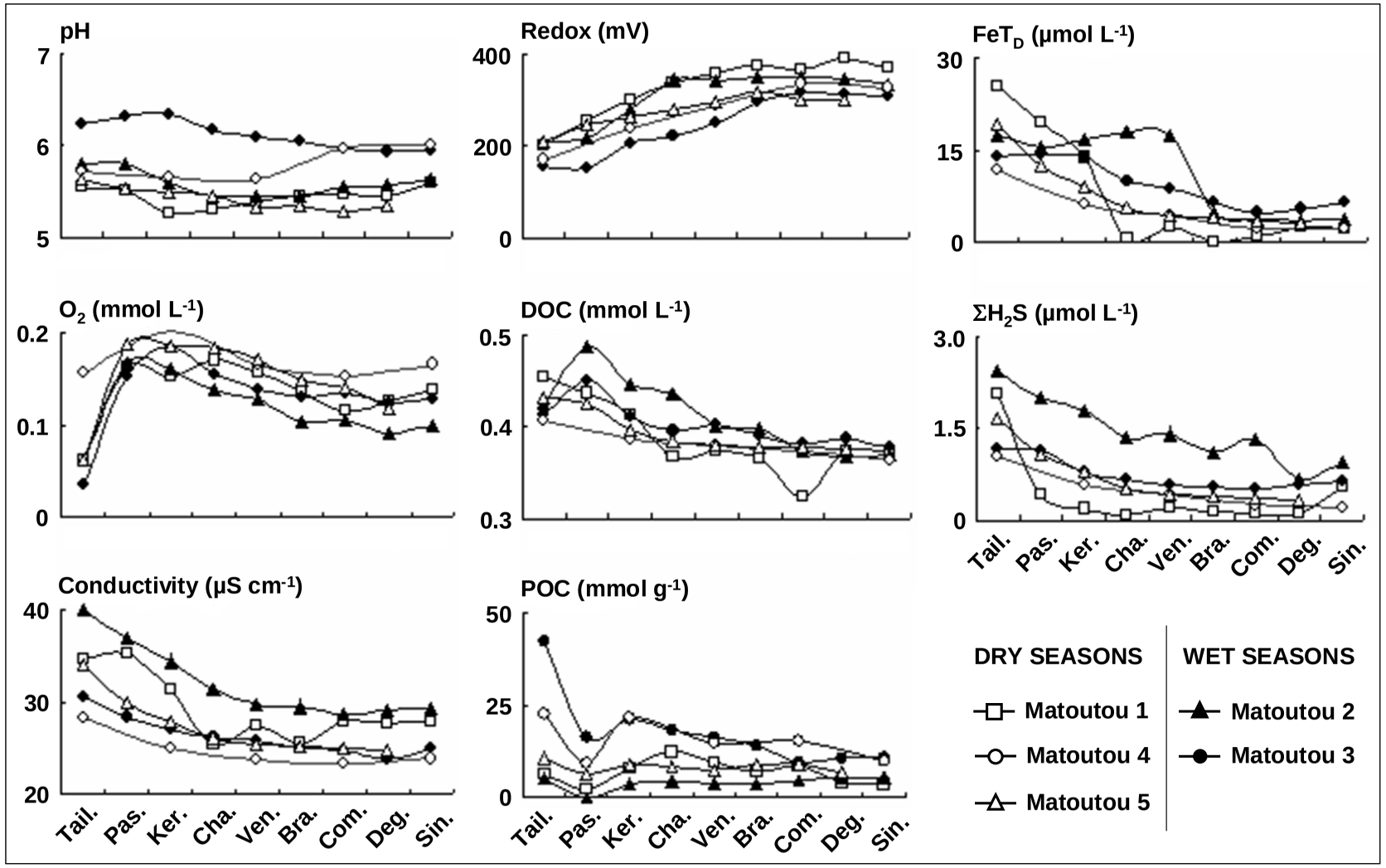

Fig. 2. Transects of physical characteristics and major chemical compounds in the USE. Each graph displays the distribution of a parameter with regard to Matoutou 1, 2, 3, 4 and 5 campaigns. Dam and LES boundaries were depicted by the Tail. and Sin. stations, respectively.

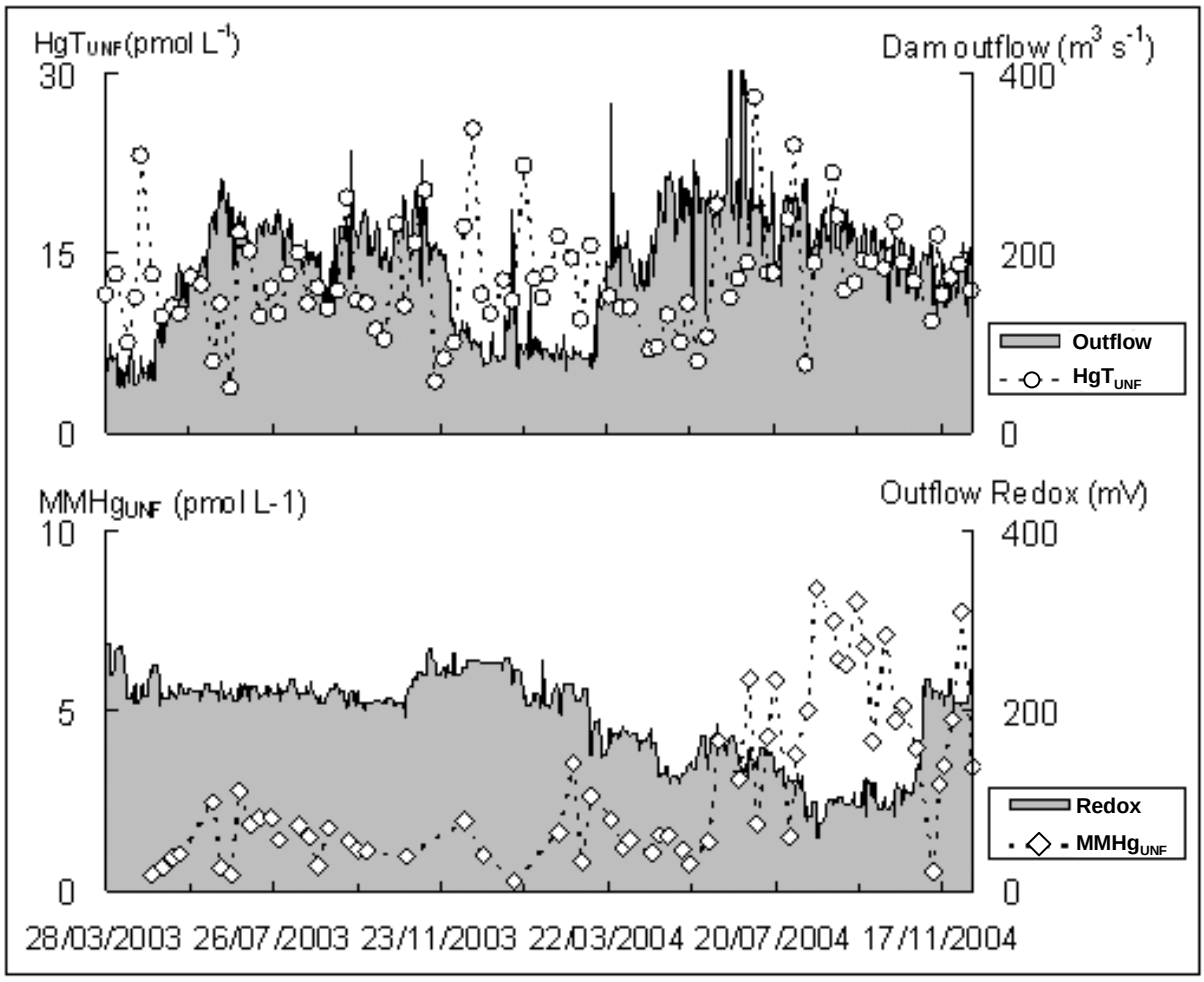

Fig. 3. Monitoring of unfiltered total (HgT_{UNF}) and monomethyl ($MMHg_{UNF}$) mercury in exported waters downstream of the dam (Tail. station). Discharge flow and associated redox were daily recorded. Samples for Hg analyses were collected on a weekly basis.

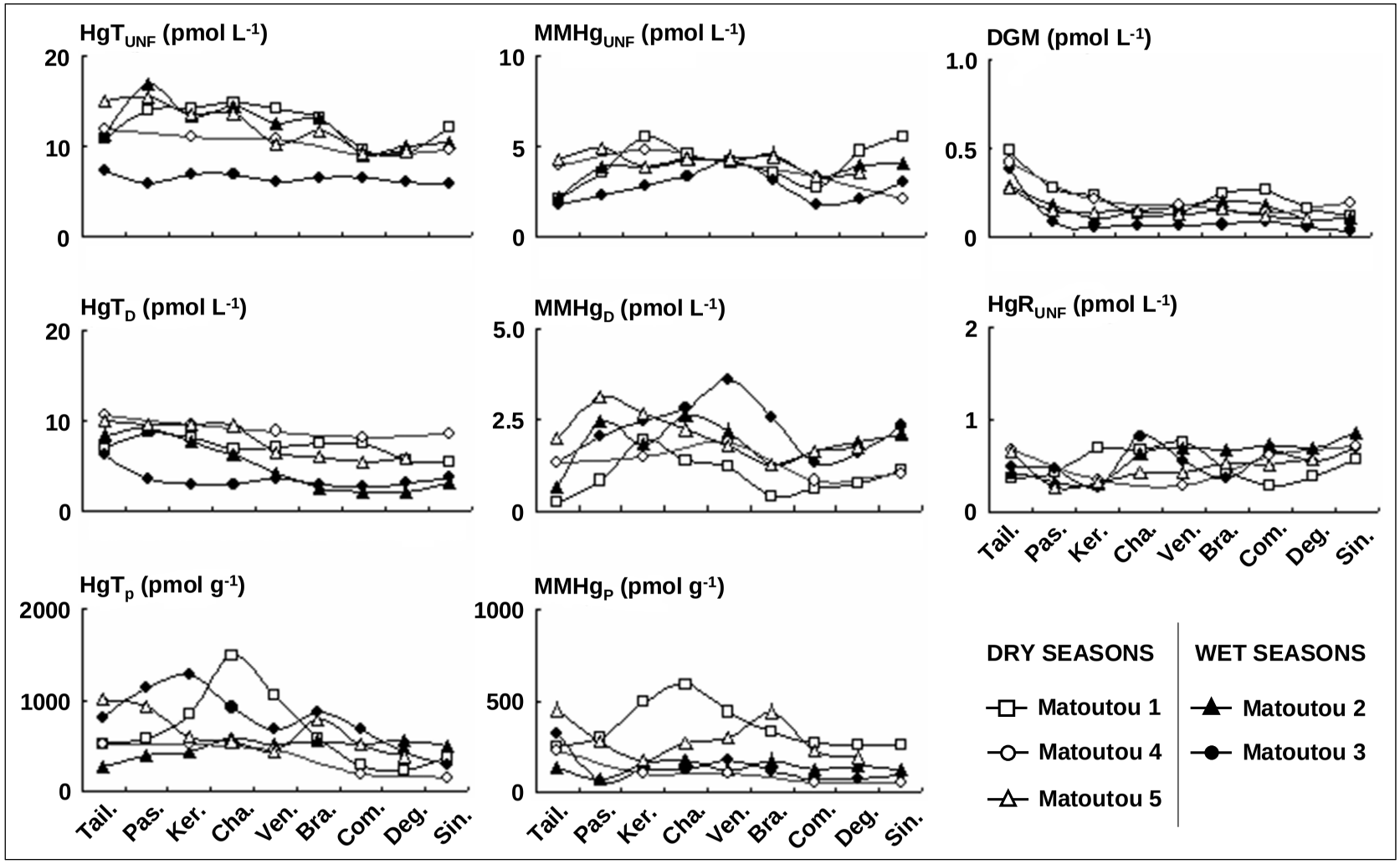

Fig. 4. Transects of main Hg species in the USE. Each graph displays the distribution of one specie with regard to Matoutou 1, 2, 3, 4 and 5 campaigns. Dam and LES boundaries were respectively depicted by the Tail. and Sin. stations.

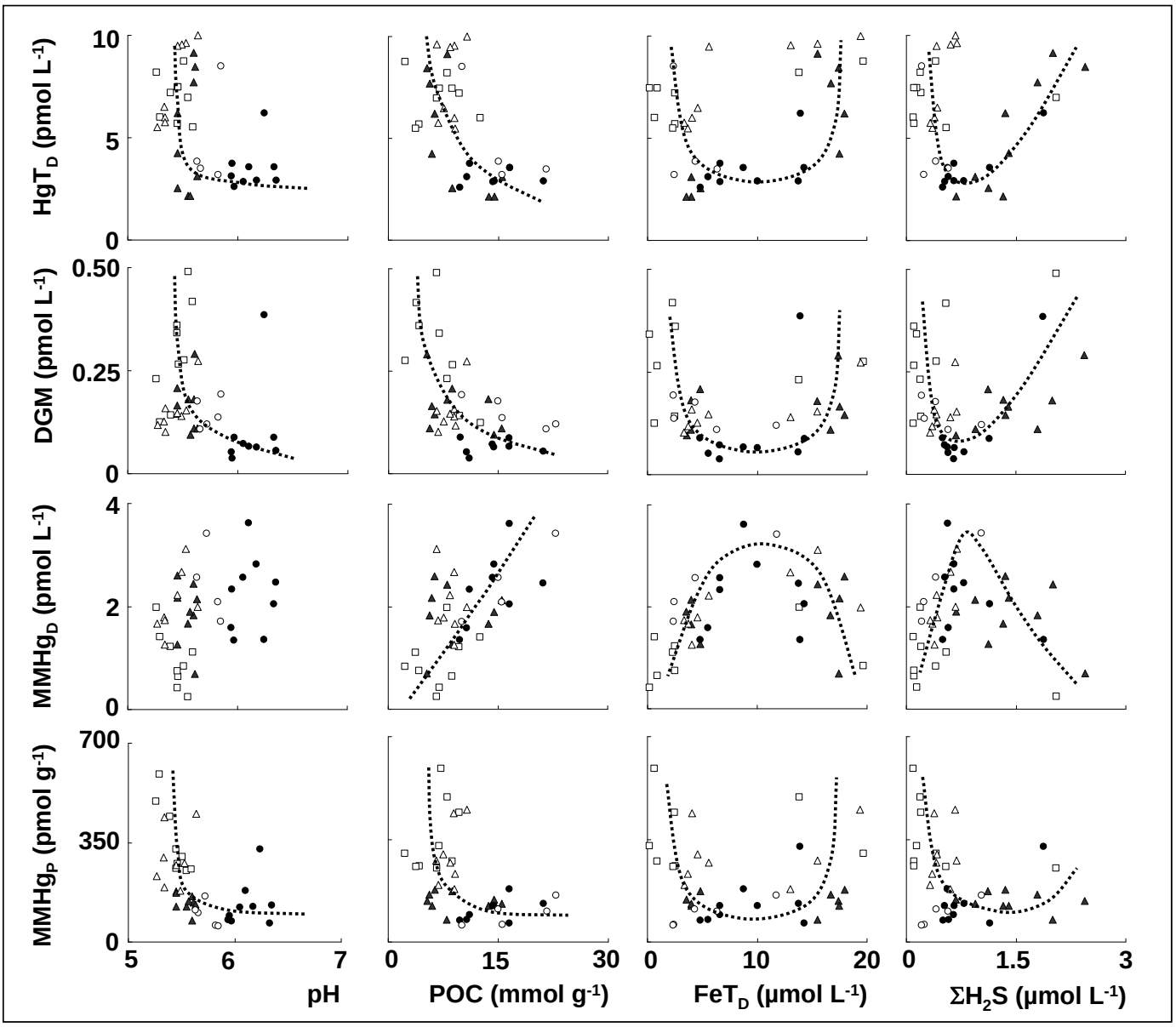

Fig. 5. Dissolved total mercury (HgT_D), dissolved gaseous mercury (DGM), dissolved and particulate monomethylmercury ($MMHg_D$) in relation to pH, particulate organic carbon (POC), dissolved total iron (FeT_D) and total sulfides (ΣH_2S). Figures were plotted using the USE data from Matoutou 1 (□), 2 (▲), 3 (●), 4 (○) and 5 (Δ) sampling campaigns.

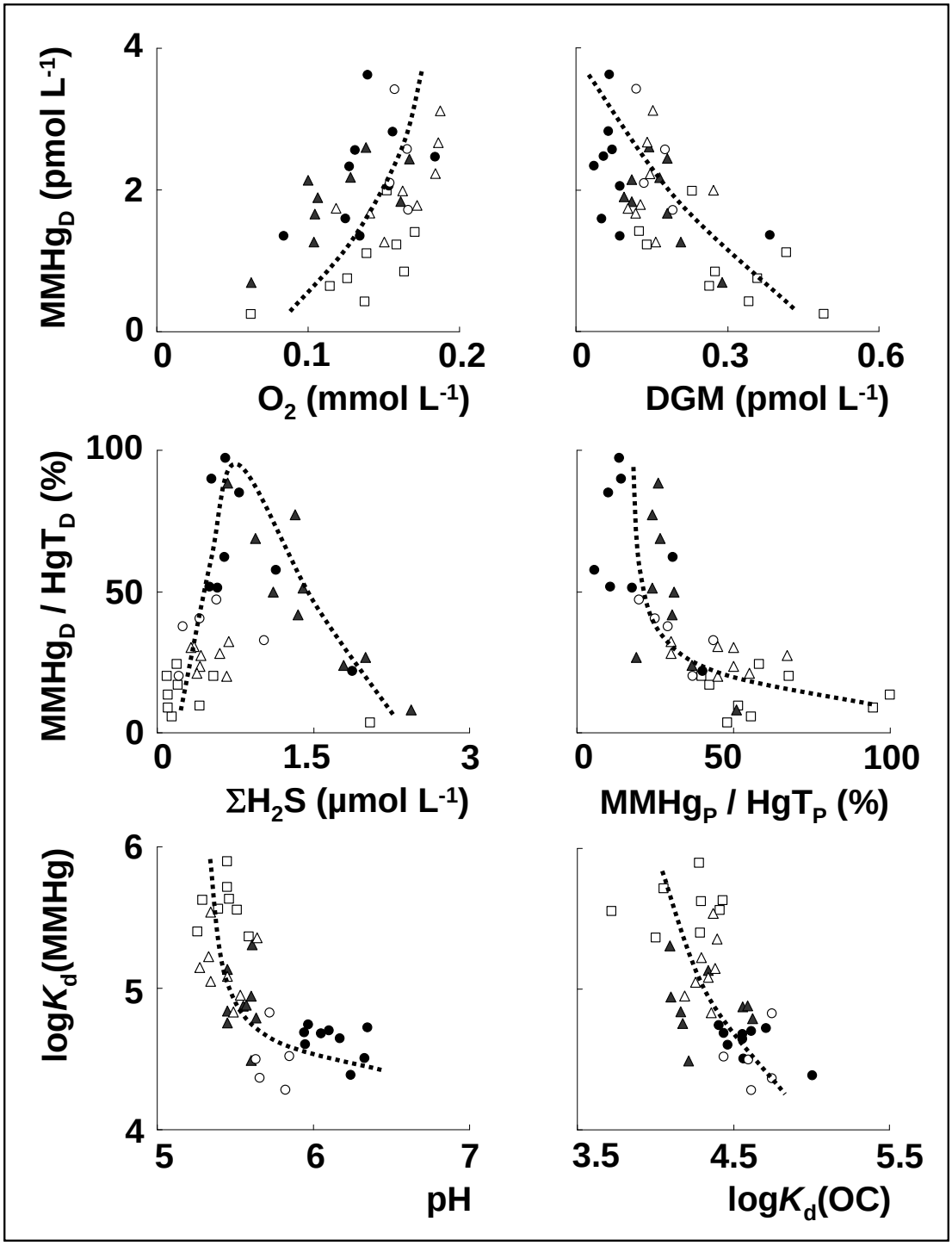

Fig. 6. Upper graphs: dissolved monomethylmercury ($MMHg_D$) as a function of dissolved oxygen (O_2) and dissolved gaseous mercury (DGM). Middle graphs: percentage of dissolved monomethylmercury [$MMHg_D/HgT_D$ (%)] in relation to total sulfides (ΣH_2S) and percentage of particulate monomethylmercury [$MMHg_P/HgT_P$ (%)]. Lower graphs: Monomethylmercury log partition coefficient [logK_d(MMHg); K_d(MMHg) = $MMHg_P/MMHg_D$] in relation to pH and organic carbon log partition coefficient [logK_d(OC); K_d(OC) = POC/DOC]. Figures were plotted using the USE data from Matoutou 1 (□), 2 (▲), 3 (●), 4 (○) and 5 (Δ) sampling campaigns.